Title: CARMA1- and MyD88-dependent activation of Jun/ATF-type AP-1 complexes is a hallmark of ABC diffuse large B-cell lymphomas.
Authors: Juilland M, Gonzalez M, Erdmann T, Banz Y, Jevnikar Z, Hailfinger S, Tzankov A, Grau M, Lenz G, Novak U, Thome M
Journal: Blood
Year: 2016 Apr 7
Volume: 127
Issue: 14
Pages: 1780-9
DOI: 10.1182/blood-2015-07-655647

CARMA1- and MyD88-dependent activation of Jun/ATF-type AP-1 complexes is a hallmark of ABC diffuse large B-cell lymphomas

Mélanie Juilland,[1] Montserrat Gonzalez,[1] Tabea Erdmann,[2,3] Yara Banz,[4] Zala Jevnikar,[1] Stephan Hailfinger,[1,*] Alexandar Tzankov,[5] Michael Grau,[6] Georg Lenz,[2,3] Urban Novak[7] and Margot Thome[1]

[1]Department of Biochemistry, University of Lausanne, Chemin des Boveresses 155, CH-1066 Epalinges, Switzerland.
[2]Translational Oncology, Department of Medicine A, Albert-Schweitzer-Campus 1, University Hospital Münster, Münster, Germany.
[3]Cluster of Excellence EXC 1003, Cells in Motion, D-48149 Münster, Germany
[4]Institute of Pathology, University of Bern, Bern, Switzerland
[5]Institute of Pathology, University Hospital Basel, Schoenbeinstrasse 40, CH-4031, Basel, Switzerland
[6]Department of Physics, Philipps-University Marburg, Renthof 5, D-35032 Marburg, Germany.
[7]Department of Medical Oncology, Inselspital, Bern University Hospital, Bern, Switzerland.

[*], present affiliation: Interfaculty Institute for Biochemistry, University of Tübingen, D-72076 Tübingen, Germany

Address correspondence to Margot Thome:

Dr. Margot Thome
Department of Biochemistry, University of Lausanne
Chemin des Boveresses 155, CH-1066 Epalinges, Switzerland
Tel.: +41-21-692.57.37
Fax: +41-21-692.57.05
E-mail: Margot.ThomeMiazza@unil.ch

Running title: AP-1 activation in ABC DLBCL

Scientific section designation: LYMPHOID NEOPLASIA

Key points

- AP-1 complexes of the Jun/ATF type promote growth of ABC DLBCL cell lines
- High expression of ATF3 is a hallmark of samples from patients with non-GC/ABC DLBCL

Abstract

A hallmark of the diffuse large B-cell lymphoma (DLBCL) of the activated B-cell (ABC) type, a molecular subtype characterized by adverse outcome, is constitutive activation of the transcription factor NF-κB, which controls expression of genes promoting cellular survival and proliferation. Much less, however, is known about the role of the transcription factor AP-1 in ABC DLBCL. Here we show that AP-1, like NF-κB, was controlled by constitutive activation of the B-cell receptor and/or toll-like receptor signaling pathways in ABC DLBCL cell lines. In contrast to germinal center B-cell (GCB) DLBCL, ABC DLBCL cell lines expressed high levels of the AP-1 family members c-Jun, JunB and JunD, which formed heterodimeric complexes with the AP-1 family members ATF2, ATF3 and ATF7. Inhibition of these complexes by a dominant negative approach led to impaired growth of a majority of ABC DLBCL cell lines. Individual silencing of c-Jun, ATF2 or ATF3 decreased cellular survival, and revealed a c-Jun/ATF2-dependent control of ATF3 expression. As a consequence, ATF3 expression was much higher in ABC versus GCB DLBCL cell lines. Samples derived from DLBCL patients showed a clear trend towards high and nuclear ATF3 expression in nodal DLBCL of the non-GC, or ABC subtype. These findings identify the activation of AP-1 complexes of the Jun/ATF-type as an important element controlling the growth of ABC DLBCL.

Introduction

Diffuse large B-cell lymphoma (DLCBL) is the most frequent form of lymphoid cancer, accounting for 30-35% of all nodal lymphomas.[1] Based on gene expression profiling (GEP), three distinct subtypes of DLBCL have been identified, namely the germinal center B-cell (GCB), activated B-cell (ABC) and primary mediastinal B-cell lymphoma subtypes.[2] The ABC subtype of DLBCL is characterized by adverse prognosis and constitutive activation of the transcription factor NF-κB.[3] This is thought to be the consequence of somatic mutations in the genes encoding the B-cell receptor (BCR)-associated CD79A and CD79B chains,[4] or the BCR signal transducer CARMA1 (also known as CARD11),[5] and polymorphisms in *RNF31* (also known as *HOIP*),[6] which result in constitutive BCR signaling. These can be present alone or in combination with activating mutations in genes encoding the Toll like receptor (TLR) downstream signaling protein MyD88[7] and inactivation and/or deletion of the gene encoding A20, a negative regulator of the NF-κB pathway.[8] As a consequence of these mutations, ABC DLBCL have a constitutive activation of NF-κB via BCR- and/or TLR-signaling pathways, whose natural physiological role is to promote B-cell proliferation and survival.[1]

Natural engagement of the antigen receptor, or of TLRs, activates not only NF-κB, but also transcription factors of the AP-1 family.[9,10] However, little is known about the relevance of the AP-1 transcription factor family and the molecular pathways triggering its activation leading to pathology of ABC DLBCL. The AP-1 family comprises hetero- and homo-dimeric transcription factors that are formed by combinations of members of the Jun, Fos, ATF and Maf subfamilies.[11] AP-1 dimers have different DNA recognition sequences and are also differentially regulated according to the cell type and/or activating stimulus. Various posttranslational modifications can modulate AP-1 activity, by controlling the abundance and the activity of the individual dimers.[12] Ser/Thr kinases of the MAPK family, in particular ERK and JNK, have been shown to phosphorylate c-Fos and c-Jun and to thereby control their stability and activity.[11] Antigen receptor triggering leads to induction and/or activation of multiple AP-1 family members, including c-Fos, c-Jun, JunB, ATF2 and ATF3, but the individual roles of these AP-1 family transcription factors for lymphocyte proliferation remain poorly understood. [11,13-17]

Recent studies have provided some insight into how the BCR and the TLR signaling pathways activate gene transcription via the AP-1 pathway.[18] BCR signaling depends on the CARMA1-BCL10-MALT1 (CBM) complex, while TLR signaling depends on the adaptor protein MyD88 and the kinases IRAK1 and IRAK4. The ubiquitin ligase TRAF6 and the Ser/Thr kinase TAK1 are downstream targets of both, BCR/CBM- and TLR/MyD88/IRAK-dependent signals. TAK1 has been reported to act as an upstream regulator of the c-Jun N-terminal kinase, JNK,[19-22] it is thus generally assumed that BCR- and TLR-induced JNK activation is crucial for AP-1 activation. However, the exact role of JNK in the activation of individual AP-1 family heterodimers in lymphocytes remains incompletely understood, and whether JNK is strictly required for AP-1 activation in lymphocytes remains controversial. [23-26] Another particular difficulty in studying the role of AP-1 transcription factors is the fact that the AP-1 family comprises more than 20 members that can form numerous different heterodimers with partially redundant functions and highly diverse mechanisms of regulation.[11] Therefore, little is currently known about the exact composition and relevance of AP-1 complexes in activated lymphocytes and the development of ABC DLBCL.

Here, we show that cell lines derived from ABC DLBCL are characterized by constitutive upregulation of c-Jun, JunB and ATF3, which was mediated by CARMA1 and MyD88. Jun members formed complexes with ATF2 or ATF7 (complexes of type I), or with ATF3 (complexes of type II). Inhibition of these complexes by a dominant negative approach impaired the viability of most ABC DLBCL cell lines. Amongst the different members of the complexes, ATF3, ATF2 and c-Jun were the main drivers of cellular survival. Interestingly, ATF3, but not ATF2 or ATF7, was exclusively expressed in cell lines derived from the ABC subtype of DLBCL, and immuno-histochemical analysis of biopsies of DLBCL patients confirmed preferential strong and nuclear ATF3 staining in samples from patients with nodal lymphoma of the non-GC or ABC subtype of DLBCL. Collectively, these findings identify the activation of specific AP-1 complexes as a hallmark of ABC DLBCL.

Methods

Cellular transfection and transduction

Lentiviral transduction and viability assays have been described.[28] Expression of A-Fos in DLBCL lines was achieved by retroviral transduction as described previously[29]. The transduced cells were monitored for live GFP^+ cells by flow cytometry as described.[30]

Cell culture, cell stimulation and reporter assays

Jurkat cells and DLBCL cell lines BJAB, SUDHL-4, SUDHL-6, HT, HBL-1, OCI-Ly3, OCI-Ly10 and TMD8 were cultured as described.[30] For stimulation of Jurkat T cells, a mixture of PMA (phorbol 12-myristate 13-acetate; 10 ng/ml; Alexis) and ionomycin (1 μM; Calbiochem) was used. In some experiments, cells were preincubated with 1 μM of the JNK inhibitor SP600125 (Calbiochem), 1 μM of TAK1 inhibitor 5Z7 (Sigma), PKC inhibitors (500 nM bisindoleylmaleimide VIII acetate (Alexis) or 1 μM of Gö6976 (Calbiochem)) or with corresponding volumes of solvent for the indicated times at 37°C. IL-2 luciferase assays were performed as described.[28]

Cell lysis, immunoprecipitation and Western blot analysis

Cells were lysed in RIPA buffer containing 50 mM Tris-HCl, pH 7.4, 1% NP-40, 0.25% sodium deoxycholate, 150 mM NaCl and 1mM EDTA, or in lysis buffer containing 50 mM HEPES, pH 7.5, 150 mM NaCl, 1% Triton X-100, protease inhibitors (Complete; Roche) and phosphatase inhibitors (NaF, $Na_4P_2O_7$ and Na_3VO_4). In some experiments, lysates were incubated with or without 0.5 mM BS3 (Thermo Scientific) for 1h at 4°C. Immunoprecipitation, sample analysis by high resolution SDS-PAGE and immunoblot were performed as described.[28]

Patient populations

The construction of the tissue microarray (TMA) with samples from de novo previously untreated DLBCL patients classified by the Hans algorithm[31] has been described elsewhere.[32] Of the original cohort of 109 patients, sufficient tumor tissue for additional immunohistochemical analyses was available from 70 patients. The local ethics committee approved this retrospective analysis (KEK 160/14). A second

cohort of DLBCL patients consisted of a GEP-characterized subset of a patient cohort already published.[29] The study of this cohort was approved by the ethics committee of Northwestern and Central Switzerland (EKNZ 2014-252).

Immunohistochemistry for ATF3

Immunohistochemical staining of the ATF3 protein was performed on the TMA slides using an automated immunostainer (Leica BOND-III, Leica Biosystems). As a pretreatment for antigen retrieval, the TMA section was placed in epitope retrieval solution (Tris buffer for 30 min at 95°C). Subsequently, the TMA was incubated at room temperature with rabbit anti-human ATF3 antibody (sc-188, Santa Cruz) at a working concentration of 1:50 for 30 min. Antigen detection was performed using a commercial detection kit (Bond Polymer Refine Detection) with diaminobenzidin as the chromogen.

Immunohistochemical scoring

For assessment of ATF3 expression, the stained TMA slides were scanned with Aperio (Vista, USA) and evaluated at 40x magnification. The staining intensity was stratified from 0 – 2, where 0 (designated “weak”) = negative or weak staining in <10% of neoplastic cells, 1 (designated “intermediate”) = weak or moderate staining in >10% neoplastic cells and 2 (designated “strong”) = strong staining in >10% of neoplastic cells. Staining was further categorized by its pattern as partially or predominantly nuclear (N) or cytoplasmic (C). Staining intensity was semi-quantitative and used internal samples as reference points.

Plasmids, antibodies, mass spectrometry and fluorescence microscopy

Detailed information about plasmids, antibodies, mass spectrometry and fluorescence microscopy can be found in the supplemental material.

Statistical analysis

Two-tailed Student's t-test was used for statistical analysis; P values of 0.05 or less were considered statistically significant.

Results

Jun family proteins are upregulated in ABC DLBCL cell lines in a CARMA1/MALT1- and MyD88/IRAK-dependent manner

To assess whether AP-1 family members are differentially expressed in ABC versus GCB DLBCL, we first monitored the expression of different Jun family members in four cell lines derived from each of the two DLBCL subtypes. Interestingly, c-Jun and JunB protein levels were clearly higher in all ABC DLBCL cell lines compared to GCB DLBCL cell lines (**Figure 1A**), consistent with a recent report.[18] In addition, JunD levels were generally higher in ABC DLBCL cell lines (**Figure 1A**). Most of the cell lines derived from ABC DLBCL, including all four cell lines used in this study, have somatic mutations driving constitutive BCR/CBM- or TLR/MyD88-dependent signaling.[4,5,7,8,33] We thus subsequently assessed the individual requirement of these pathways for the expression of Jun family members. Expression of c-Jun and JunB, but not of JunD, was clearly dependent on constitutive CBM- and MyD88-dependent constitutive signaling, as evident from the observed reduction of c-Jun and JunB expression upon silencing of CARMA1, MALT1, MyD88 or IRAK1 (**Figure 1B**). Consistent with a critical role of PKC family kinases downstream of CD79 and upstream of CARMA1,[34-36] we observed a reduction of cellular c-Jun protein expression in all ABC DLBCL cell lines with CD79 mutations (HBL-1, OCI-Ly10 and TMD8) upon pretreatment with the pan-PKC inhibitor bisindolyl-maleimide VIII (BIM VIII) or the more selective inhibitor of classical PKC isoforms, Gö6976, with the exception of the HBL-1 cells, which did not react to Gö6976 (**supplemental Figure 1A**).

c-Jun and JunB expression requires TAK1 activity

The exact molecular mechanism that controls JunB and JunD upregulation in lymphocytes is unknown. c-Jun, however, is stabilized by phosphorylation on Ser residues 63 and 73, which inhibits its otherwise constitutive proteasomal degradation.[37,38] Accordingly, the increased levels of c-Jun expression in ABC DLBCL cell lines correlated with constitutive c-Jun phosphorylation on Ser 63 (**Figure 1A**). Since phosphorylation on Ser 63 has been described to be a target of phosphorylation by the MAPK JNK,[37,38] we analyzed the activation status of the MAPK JNK, as well as other MAPKs such as p38 and ERK. We detected constitutive

JNK, p38 and ERK activation in several ABC and GCB DLBCL cell lines (**Figure 1C**), in agreement with recently reported findings.[39] However, we saw no obvious correlation between MAPK activation and c-Jun phosphorylation and accumulation (compare **Figure 1A** and **1C**). When pretreating the DLBCL cell lines with the JNK inhibitor SP600125, at a concentration that efficiently prevented PMA/ionomycin-induced c-Jun accumulation in Jurkat T cells (**supplemental Figure 1B**), we observed a clear reduction of c-Jun levels only in the ABC DLBCL cell line HBL-1 (**supplemental Figure 1C**). Thus, JNK activation is unlikely to be a common driving factor of c-Jun phosphorylation on Ser 63, which is a specific feature of ABC DLBCL cell lines. In contrast, pretreatment of the cells with an inhibitor of the Ser/Thr kinase TAK1, 5Z7, which has been reported to act as a downstream signaling component of antigen receptor and TLR-induced signaling and an upstream regulator of JNK,[19-22] efficiently reduced c-Jun expression levels and phosphorylation in all ABC DLBCL cell lines tested (**Figure 1D**). The TAK1 inhibitor also affected JunB levels in 3 out of 4 ABC cell lines, while it had little, or no effect, on JunD levels (**Figure 1D**). Thus, cell lines derived from ABC DLBCL have high levels of JunB and c-Jun expression and c-Jun phosphorylation. Whether this is mediated directly or indirectly by TAK1 and/or a TAK1-dependent kinase remains to be identified.

Jun family members form constitutive type I complexes with ATF2 or ATF7 in ABC and GCB DLBCL cell lines

AP-1 family members can form homo- or heterodimeric complexes, typically by association of two AP-1 family members of the Jun, Fos, ATF and Maf subfamilies.[11] To gain additional insight into the biochemical composition of AP-1 complexes formed by c-Jun, JunB and JunD in ABC DLBCL cell lines, we performed chemical cross-linking experiments. Upon treatment of cell lysates with the chemical cross-linker BS3, we observed that all three Jun family members formed two different types of higher molecular weight complexes, subsequently called complexes of type I or II (**Figure 2A**). The observed distinct shifts in the relative molecular weight of the Jun-binding complexes suggested that these contained Jun-binding partners of two distinct molecular weights. For c-Jun, type I complexes tended to be more abundant in ABC than in GCB DLBCL cell lines, while formation of type II complexes was a distinct feature of all Jun family members specifically observed in ABC, but not in GCB DLBCL cell lines. By mass spectrometry, we identified ATF2 and ATF7 as specific

components of type I complexes of c-Jun in HBL-1 cells (**Figure 2B** and **supplemental Table 1**), suggesting that type I complexes contain both, c-Jun/ATF2 and c-Jun/ATF7 heterodimers. ATF2 and ATF7 expression levels were similar in all ABC and GCB cell lines tested, with the exception of HBL-1 cells, which had slightly higher ATF2 expression levels (**Figure 2C**). Cross-linking of lysates using BS3 revealed that ATF2 and ATF7 formed high molecular weight complexes in both GCB and ABC DLBCL cell lines, and that these complexes corresponded in molecular weight to type I complexes (**Figure 2D**). Association of ATF2 and ATF7 with c-Jun, JunB and JunD was confirmed by co-immunoprecipitation assays performed on two ABC and two GCB DLBCL cell lines (**Figure 2E**). Amongst these, c-Jun complexes with ATF2 and ATF7 were more abundant in ABC than in GCB DLBCL cell lines (**Figure 2E**). Thus, the Jun family members c-Jun, JunB and JunD form constitutive complexes with ATF2 or ATF7 (type I complexes, **Figure 2F**) in both, ABC and GCB DLBCL cell lines. However, c-Jun-containing type I complexes were more abundant in ABC DLBCL cell lines (**Figure 2, A and E**).

ATF3 is specifically upregulated and forms type II complexes with Jun family members in ABC DLBCL cell lines

Protein components present in type II complexes were not sufficiently abundant to be identified by mass spectrometry. However, based on the relative molecular weight of the chemically cross-linked type II complexes, we hypothesized that these may correspond to lower molecular weight members of the ATF subfamily, such as ATF3 and JDP2. In line with this idea, we found that ATF3 was specifically expressed in cell lines derived from ABC, but not from GCB DLBCLs (**Figure 3A**). In contrast, the unconventional ATF family member JDP2, which acts as a repressor of ATF2 and ATF3 function,[40,41] was less abundant in three out of four ABC as compared to GCB DLBCL cell lines. JDP2 has been shown to be targeted for proteasomal degradation upon its phosphorylation.[42] Indeed, all ABC DLBCL cell lines were characterized by the presence of an additional slower-migrating, phosphatase-sensitive isoform of JDP2 (**Figure 3A**, and data not shown), suggesting that JDP2 is constitutively phosphorylated and targeted for proteasomal degradation in ABC DLBCL cell lines.

As for c-Jun and JunB, the expression of ATF3 was strongly reduced upon silencing of CARMA1, MALT1, IRAK1 and MyD88 (**Figure 3B**). Upon treatment with the chemical cross-linker BS3, ATF3 shifted towards a higher molecular weight

complex that corresponded in size to the previously described type II complexes (**Figure 3C**). Moreover, ATF3 could easily be co-immunoprecipitated with c-Jun, JunB and JunD in lysates of ABC DLBCL cell lines (**Figure 3D**). Collectively, these findings suggest that the AP-1 family member ATF3 is selectively expressed in cell lines derived from ABC DLBCL, and forms constitutive complexes with c-Jun, JunB and JunD (type II complexes, **Figure 3E**) in these cells.

Inhibition of Jun family members by A-Fos impairs the viability of cell lines derived from ABC DLBCL.

To explore the role of Jun/ATF-type dimers in ABC DLBCL, we made use of a previously described dominant negative A-Fos construct.[43] A-Fos contains the Jun-binding leucine zipper region of c-Fos fused to a negatively charged protein domain that binds to, and thereby, masks the positively charged DNA-binding domain of c-Jun (**Figure 4A**). When stably expressed in Jurkat T cells, the A-Fos construct bound to c-Jun, JunB and JunD in both, unstimulated and PMA/ionomycin-stimulated cells (**Figure 4B**), and efficiently inhibited the inducible expression of an IL-2 luciferase reporter gene (**Figure 4C**), which is known to be AP-1 dependent.[44] We then transduced DLBCL cell lines with a retroviral construct allowing the co-expression of A-Fos with green fluorescent protein (GFP), to specifically monitor the viability of GFP^+, A-Fos expressing cells. Compared to a dominant negative IκB (DN-IκB) construct, which inhibits the NF-κB transcriptional pathway and rapidly affects the viability of ABC DLBCL cell lines, A-Fos expression led to a slow reduction in cell viability in three out of four ABC DLBCL cell lines tested (**Figure 4D**). No impact on cell viability was observed for GCB DLBCL cell lines transduced with either DN-IκB or A-Fos (**Figure 4D**). To further explore the role of individual ATF family members, we silenced the expression of ATF2, ATF3 and ATF7 in HBL-1 cells and monitored cell survival (**Figure 4, E and F**). Under these conditions, ATF3 silencing affected cell survival to an extent that was similar to that previously seen with A-Fos (**Figure 4E**). Silencing of ATF7 had little effect on survival, while ATF2 silencing clearly affected cell survival (**Figure 4F**). However, silencing of ATF2 simultaneously diminished the expression of ATF3, suggesting that the effect of ATF2 silencing on cell viability may be indirectly mediated by ATF3 (**Figure 4F**). Collectively, this suggests that ATF3-containing type II complexes have a major role in cell survival,

and that ATF2-containing type I complexes most likely contribute to cell survival indirectly by affecting ATF3 levels. Silencing of c-Jun, the major component of type I complexes in ABC DLBCL cell lines (**Figure 2, A and E**), also had a clear impact on both cell viability and ATF3 expression in HBL-1 cells (**supplemental Figure 2**). Together with our biochemical data (**Figure 2, A and E**), these findings suggest that c-Jun/ATF2-dependent ATF3 expression is relevant for the viability of a majority of ABC DLBCL cell lines.

Strong nuclear ATF3 expression characterizes nodal tumors from non-GC/ABC DLBCL patients.

To validate the relevance of our cell line-based findings, we first assessed the expression of ATF3 in tissue samples from a cohort of 350 patient samples classified by GEP.[45] At the mRNA level, expression of ATF3, but not of ATF2 or ATF7, was significantly higher in patients with ABC versus GCB DLBCL (**Figure 5A**). Subsequently, we assessed ATF3 expression in DLBCL samples by immunohistochemistry (IHC). To this purpose, staining conditions for ATF3 were optimized in DLBCL cell lines to detect strong staining in all four ABC DLBCL cell lines tested, and only minimal background staining in GCB DLBCL cell lines (**Figure 5B**). We then analysed samples of two different cohorts of DLBCL patients for ATF3 expression, which was scored according to the intensity (weak, intermediate or strong; for scoring details, see materials and methods) and the preferential localisation (cytoplasmic (C), exclusively or partially nuclear (N)). First, we analysed a cohort of 70 DLBCL samples, which were classified into GCB and non-GC DLBCL according to the Hans algorithm,[32] and were derived from 28 nodal and 42 extranodal tumors. These IHC analyses showed various expression patterns, which differed in intensity and staining pattern, examples of these are shown in **Figure 5C**. When scoring ATF3 expression intensities and patterns in the combined samples, we observed a small tendency towards higher and nuclear expression in non-GC versus GCB samples (**supplemental Figure 3**). This tendency was striking in samples obtained from nodal tumors (**Figure 5D**). In contrast, no such tendency was present in samples from extranodal tumors (data not shown), most likely because the Hans algorithm has been established and validated only for nodal DLBCL. Interestingly, in gastric DLBCL the Hans and another algorithm failed in identifying prognostically relevant subgroups[46] . Furthermore, extranodal DLBCL outside the testicles and the CNS more commonly

encompass morphologically and clinically unrecognizable transformed marginal zone B-cell lymphomas, for which an algorithm has not been developed. We also analysed a second cohort of 17 nodal DLBCL samples, which were classified into the GCB or ABC subtype according to GEP.[29] Amongst these, ATF3 expression was strong in 7/9 samples and intermediate in 2/9 ABC DLBCL, while GCB DLBCL showed negative or intermediate expression levels in 7/8 samples and strong staining was observed in only one GCB DLBCL sample (**Fig. 5E**). In the majority of non-GC DLBCL samples (14 out of 19), or GEP-identified ABC DLBCL samples (6 out of 9), the ATF3 staining was partially or predominantly nuclear. Collectively, these data identify high and preferentially nuclear protein expression of ATF3 as a hallmark of human non-GC/ABC DLBCL.

Discussion

In the present study, we demonstrated a new and essential role for the activation of the Jun/ATF branch of the AP-1 pathway in the growth of ABC DLBCL, and identified strong ATF3 expression as a hallmark of this cancer. When exploring the molecular causes of AP-1 activation in ABC DLBCL, we observed that c-Jun, JunB and JunD levels were systematically upregulated in ABC DLBCL cell lines, and that c-Jun and JunB upregulation occurred in a CARMA1/MALT1- or MyD88/IRAK-1 dependent manner. Recent studies have shown that CARMA1 can drive c-Jun and JunB expression,[18] and promote AP-1 activation via the adaptor protein BCL10, which recruits MEKK7 to promote JNK2-mediated c-Jun phosphorylation and stabilization.[47] We extend these findings and show that constitutive activation of MyD88 and IRAK also contributes to the increased expression of these AP-1 family members in ABC DLBCL cell lines. However, and consistent with a recent study,[39] we saw no correlation of JNK activation with c-Jun upregulation in ABC DLBCL (except for HBL-1 cells). Instead, we found that JunB expression and c-Jun phosphorylation and expression were efficiently blocked by inhibition of the Ser/Thr kinase TAK1. Therefore, TAK1 may directly or indirectly control c-Jun and JunB stability.

Using biochemical approaches, we explored the molecular composition of AP-1 complexes in DLBCL cell lines, and identified ATF2, ATF7 and ATF3 as specific constitutive binding partners of c-Jun, JunB and JunD. Interestingly, c-Jun/ATF2- and c-Jun/ATF7-containing complexes were generally much more abundant in ABC

DLBCL cell lines, and ATF3-containing AP-1 heterodimers with c-Jun, JunB or JunD were identified as a selective feature of ABC DLBCL cell lines. Using a dominant negative A-Fos construct or shRNA-mediated silencing of individual AP-1 components, we demonstrated that Jun/ATF-type complexes are important drivers of the proliferation of DLBCL cell lines. These findings are consistent with a previously proposed role for Jun/ATF complexes in conducting autocrine cell growth in other malignancies.[48]

In the present study, we have attained a better understanding of the molecular mechanisms driving high expression of ATF3 in ABC DLBCL. An important aspect of the regulation of ATF3 levels was its transcriptional upregulation in ABC DLBCL, which was controlled by c-Jun and ATF2. Indeed, the ATF3 promotor has been previously shown to be a c-Jun/ATF2-target in HeLa cells.[49] Therefore, high levels of ATF3 are most likely maintained in ABC DLBCL cells by a positive feedback loop. Additionally, our finding of constitutive phosphorylation of JDP2 in ABC as compared to GCB DLBCL cell lines may provide another explanation for the increased levels of ATF3 in the ABC DLBCL subtype. JDP2 binds the ATF3 promotor and suppresses ATF3 transcription, and phosphorylation has been reported to control JDP2 protein stability.[42] Understanding of the mechanism underlying constitutive JDP2-phosphorylation and –turnover, and of its relevance for cellular transformation in ABC DLBCL will be an interesting aspect of future studies.

ATF3 has been described to have controversial roles in either oncogenesis or tumor suppression in diverse tumor models.[50] These seemingly conflicting roles depend on the type of ATF3 homo-or heterodimers formed, which have different DNA binding specificities, and thus on the expression and activity of individual ATF3 binding partners in the cellular context.[50] In ABC DLBCL, ATF3 was highly expressed and constitutively bound to c-Jun, JunB or JunD, suggesting an important role for Jun/ATF3 heterodimers in lymphomagenesis that is consistent with several previous studies highlighting a proliferation-promoting and/or cell-transforming role for ATF3.[51-54] We consistently observed a tendency towards strong and nuclear ATF3 expression in samples from patients with ABC DLBCL that were classified either by the Hans algorithm or by GEP. Interestingly, high constitutive ATF3 expression has also been described for Hodgkin lymphoma cells, which depend on ATF3 expression for viability,[55] and in adult T-cell leukemia cells,[56] suggesting that ATF3 promotes different types of lymphomas by a common mechanism. In conjunction with these

data, our findings support an important oncogenic role for ATF3 expression in ABC DLBCL that could be of diagnostic relevance and may inspire novel therapeutic strategies to interfere with ABC DLBCL by targeting the function and/or expression of specific AP-1 family members.

Acknowledgments

We thank Cristian Smulski for technical advice, Slavica Masina for grammatical revision of the manuscript, Manfredo Quadroni (Protein Analysis Facility, Center for Integrative Genomics, University of Lausanne) for sample analysis by mass spectrometry, and Prof. Inti Zlobec and the team of the translational research unit of the institute of pathology at the University of Bern for technical assistance with the immunohistochemical staining of human samples. This work was supported by grants of the Swiss Cancer League and the Stiftung zur Krebsbekämpfung (to M.T.) and a SNSF Sinergia grant (CRSII3_147620, to M.T. and G.L.). G.L. acknowledges additional support by Deutsche Krebshilfe, the Else-Kröner-Fresenius Stiftung and the Deutsche Forschungsgemeinschaft (DFG EXC 1003 Cells in Motion).

Authorship contributions

M.J. conceived and designed the project, performed experiments, analyzed data, and wrote the paper; M.Go., Z.J., Y.B. and T.E. performed experiments, analyzed data and revised the manuscript; U.N. and A.T. provided clinical samples and revised the manuscript; S.H. contributed to the study design and revised the manuscript; G.L. contributed to the study design, provided clinical samples, analyzed data and revised the manuscript; M.Gr. provided statistical analysis of mRNA expression data from a patient cohort; and M.T. conceived and designed the project, analyzed data and wrote the paper.

Disclosure of conflicts of interest

The authors declare no competing financial interests.

References

1. Roschewski M, Staudt LM, Wilson WH. Diffuse large B-cell lymphoma-treatment approaches in the molecular era. *Nat Rev Clin Oncol*. 2014;11(1):12-23.
2. Alizadeh AA, Eisen MB, Davis RE, et al. Distinct types of diffuse large B-cell lymphoma identified by gene expression profiling. *Nature*. 2000;403(6769):503-511.
3. Davis RE, Brown KD, Siebenlist U, Staudt LM. Constitutive nuclear factor kappaB activity is required for survival of activated B cell-like diffuse large B cell lymphoma cells. *J Exp Med*. 2001;194(12):1861-1874.
4. Davis RE, Ngo VN, Lenz G, et al. Chronic active B-cell-receptor signalling in diffuse large B-cell lymphoma. *Nature*. 2010;463(7277):88-92.
5. Lenz G, Davis RE, Ngo VN, et al. Oncogenic CARD11 Mutations in Human Diffuse Large B Cell Lymphoma. *Science*. 2008.
6. Yang Y, Schmitz R, Mitala J, et al. Essential role of the linear ubiquitin chain assembly complex in lymphoma revealed by rare germline polymorphisms. *Cancer Discov*. 2014;4(4):480-493.
7. Ngo VN, Young RM, Schmitz R, et al. Oncogenically active MYD88 mutations in human lymphoma. *Nature*. 2011;470(7332):115-119.
8. Compagno M, Lim WK, Grunn A, et al. Mutations of multiple genes cause deregulation of NF-kappaB in diffuse large B-cell lymphoma. *Nature*. 2009;459(7247):717-721.
9. Blonska M, Lin X. CARMA1-mediated NF-kappaB and JNK activation in lymphocytes. *Immunol Rev*. 2009;228(1):199-211.
10. Kawai T, Akira S. TLR signaling. *Cell Death Differ*. 2006;13(5):816-825.
11. Eferl R, Wagner EF. AP-1: a double-edged sword in tumorigenesis. *Nat Rev Cancer*. 2003;3(11):859-868.
12. Lopez-Bergami P, Lau E, Ronai Z. Emerging roles of ATF2 and the dynamic AP1 network in cancer. *Nat Rev Cancer*. 2010;10(1):65-76.
13. Tsai EY, Jain J, Pesavento PA, Rao A, Goldfeld AE. Tumor necrosis factor alpha gene regulation in activated T cells involves ATF-2/Jun and NFATp. *Mol Cell Biol*. 1996;16(2):459-467.
14. Feuerstein N, Firestein R, Aiyar N, He X, Murasko D, Cristofalo V. Late induction of CREB/ATF binding and a concomitant increase in cAMP levels in T and B lymphocytes stimulated via the antigen receptor. *J Immunol*. 1996;156(12):4582-4593.
15. Zhang J, Salojin KV, Gao JX, Cameron MJ, Bergerot I, Delovitch TL. p38 mitogen-activated protein kinase mediates signal integration of TCR/CD28 costimulation in primary murine T cells. *J Immunol*. 1999;162(7):3819-3829.
16. Gilchrist M, Henderson WR, Jr., Clark AE, et al. Activating transcription factor 3 is a negative regulator of allergic pulmonary inflammation. *J Exp Med*. 2008;205(10):2349-2357.
17. Reimold AM, Kim J, Finberg R, Glimcher LH. Decreased immediate inflammatory gene induction in activating transcription factor-2 mutant mice. *Int Immunol*. 2001;13(2):241-248.
18. Blonska M, Zhu Y, Chuang HH, et al. Jun-regulated genes promote interaction of diffuse large B-cell lymphoma with the microenvironment. *Blood*. 2015;125(6):981-991.

19. Wan YY, Chi H, Xie M, Schneider MD, Flavell RA. The kinase TAK1 integrates antigen and cytokine receptor signaling for T cell development, survival and function. *Nat Immunol*. 2006;7(8):851-858.
20. Wang C, Deng L, Hong M, Akkaraju GR, Inoue J, Chen ZJ. TAK1 is a ubiquitin-dependent kinase of MKK and IKK. *Nature*. 2001;412(6844):346-351.
21. Sato S, Sanjo H, Takeda K, et al. Essential function for the kinase TAK1 in innate and adaptive immune responses. *Nat Immunol*. 2005;6(11):1087-1095.
22. Schuman J, Chen Y, Podd A, et al. A critical role of TAK1 in B-cell receptor-mediated nuclear factor kappaB activation. *Blood*. 2009;113(19):4566-4574.
23. Staal J, Driege Y, Bekaert T, et al. T-cell receptor-induced JNK activation requires proteolytic inactivation of CYLD by MALT1. *EMBO J*. 2011;30(9):1742-1752.
24. Jaworski M, Marsland BJ, Gehrig J, et al. Malt1 protease inactivation efficiently dampens immune responses but causes spontaneous autoimmunity. *EMBO J*. 2014;33(23):2765-2781.
25. Gewies A, Gorka O, Bergmann H, et al. Uncoupling Malt1 threshold function from paracaspase activity results in destructive autoimmune inflammation. *Cell Rep*. 2014;9(4):1292-1305.
26. Bornancin F, Renner F, Touil R, et al. Deficiency of MALT1 Paracaspase Activity Results in Unbalanced Regulatory and Effector T and B Cell Responses Leading to Multiorgan Inflammation. *J Immunol*. 2015;194(8):3723-3734.
27. Neal JW, Clipstone NA. Calcineurin mediates the calcium-dependent inhibition of adipocyte differentiation in 3T3-L1 cells. *J Biol Chem*. 2002;277(51):49776-49781.
28. Rebeaud F, Hailfinger S, Posevitz-Fejfar A, et al. The proteolytic activity of the paracaspase MALT1 is key in T cell activation. *Nat Immunol*. 2008;9:272-281.
29. Pfeifer M, Grau M, Lenze D, et al. PTEN loss defines a PI3K/AKT pathway-dependent germinal center subtype of diffuse large B-cell lymphoma. *Proc Natl Acad Sci U S A*. 2013;110(30):12420-12425.
30. Hailfinger S, Lenz G, Ngo V, et al. Essential role of MALT1 protease activity in activated B cell-like diffuse large B-cell lymphoma. *Proc Natl Acad Sci USA*. 2009;106(47):19946-19951.
31. Hans CP, Weisenburger DD, Greiner TC, et al. Confirmation of the molecular classification of diffuse large B-cell lymphoma by immunohistochemistry using a tissue microarray. *Blood*. 2004;103(1):275-282.
32. Reber R, Banz Y, Garamvolgyi E, Perren A, Novak U. Determination of the molecular subtypes of diffuse large B-cell lymphomas using immunohistochemistry: a case series from the Inselspital, Bern, and a critical appraisal of this determination in Switzerland. *Swiss Med Wkly*. 2013;143:w13748.
33. Pasqualucci L, Trifonov V, Fabbri G, et al. Analysis of the coding genome of diffuse large B-cell lymphoma. *Nat Genet*. 2011;43(9):830-837.
34. Matsumoto R, Wang D, Blonska M, et al. Phosphorylation of CARMA1 plays a critical role in T Cell receptor-mediated NF-kappaB activation. *Immunity*. 2005;23(6):575-585.
35. Sommer K, Guo B, Pomerantz JL, et al. Phosphorylation of the CARMA1 linker controls NF-kappaB activation. *Immunity*. 2005;23(6):561-574.
36. Shinohara H, Yasuda T, Aiba Y, et al. PKC beta regulates BCR-mediated IKK activation by facilitating the interaction between TAK1 and CARMA1. *J Exp Med*. 2005;202(10):1423-1431.

37. Fuchs SY, Dolan L, Davis RJ, Ronai Z. Phosphorylation-dependent targeting of c-Jun ubiquitination by Jun N-kinase. *Oncogene*. 1996;13(7):1531-1535.
38. Musti AM, Treier M, Bohmann D. Reduced ubiquitin-dependent degradation of c-Jun after phosphorylation by MAP kinases. *Science*. 1997;275(5298):400-402.
39. Schmid CA, Robinson MD, Scheifinger NA, et al. DUSP4 deficiency caused by promoter hypermethylation drives JNK signaling and tumor cell survival in diffuse large B cell lymphoma. *J Exp Med*. 2015;212(5):775-792.
40. Weidenfeld-Baranboim K, Hasin T, Darlyuk I, et al. The ubiquitously expressed bZIP inhibitor, JDP2, suppresses the transcription of its homologue immediate early gene counterpart, ATF3. *Nucleic Acids Res*. 2009;37(7):2194-2203.
41. Jin C, Ugai H, Song J, et al. Identification of mouse Jun dimerization protein 2 as a novel repressor of ATF-2. *FEBS Lett*. 2001;489(1):34-41.
42. Weidenfeld-Baranboim K, Koren L, Aronheim A. Phosphorylation of JDP2 on threonine-148 by the c-Jun N-terminal kinase targets it for proteosomal degradation. *Biochem J*. 2011;436(3):661-669.
43. Olive M, Krylov D, Echlin DR, Gardner K, Taparowsky E, Vinson C. A dominant negative to activation protein-1 (AP1) that abolishes DNA binding and inhibits oncogenesis. *J Biol Chem*. 1997;272(30):18586-18594.
44. Jain J, Loh C, Rao A. Transcriptional regulation of the IL-2 gene. *Curr Opin Immunol*. 1995;7(3):333-342.
45. Lenz G, Wright G, Dave SS, et al. Stromal gene signatures in large-B-cell lymphomas. *N Engl J Med*. 2008;359(22):2313-2323.
46. Hwang HS, Yoon DH, Suh C, Park CS, Huh J. Prognostic value of immunohistochemical algorithms in gastrointestinal diffuse large B-cell lymphoma. *Blood Res*. 2013;48(4):266-273.
47. Blonska M, Pappu BP, Matsumoto R, et al. The CARMA1-Bcl10 signaling complex selectively regulates JNK2 kinase in the T cell receptor-signaling pathway. *Immunity*. 2007;26(1):55-66.
48. van Dam H, Castellazzi M. Distinct roles of Jun : Fos and Jun : ATF dimers in oncogenesis. *Oncogene*. 2001;20(19):2453-2464.
49. Liang G, Wolfgang CD, Chen BP, Chen TH, Hai T. ATF3 gene. Genomic organization, promoter, and regulation. *J Biol Chem*. 1996;271(3):1695-1701.
50. Thompson MR, Xu D, Williams BR. ATF3 transcription factor and its emerging roles in immunity and cancer. *J Mol Med (Berl)*. 2009;87(11):1053-1060.
51. Perez S, Vial E, van Dam H, Castellazzi M. Transcription factor ATF3 partially transforms chick embryo fibroblasts by promoting growth factor-independent proliferation. *Oncogene*. 2001;20(9):1135-1141.
52. Hagiya K, Yasunaga J, Satou Y, Ohshima K, Matsuoka M. ATF3, an HTLV-1 bZip factor binding protein, promotes proliferation of adult T-cell leukemia cells. *Retrovirology*. 2011;8:19.
53. Wang A, Arantes S, Conti C, McArthur M, Aldaz CM, MacLeod MC. Epidermal hyperplasia and oral carcinoma in mice overexpressing the transcription factor ATF3 in basal epithelial cells. *Mol Carcinog*. 2007;46(6):476-487.
54. Yin X, Dewille JW, Hai T. A potential dichotomous role of ATF3, an adaptive-response gene, in cancer development. *Oncogene*. 2008;27(15):2118-2127.
55. Janz M, Hummel M, Truss M, et al. Classical Hodgkin lymphoma is characterized by high constitutive expression of activating transcription factor 3 (ATF3), which promotes viability of Hodgkin/Reed-Sternberg cells. *Blood*. 2006;107(6):2536-2539.

56. Kamioka M, Imamura J, Komatsu N, Daibata M, Sugiura T. Testican 3 expression in adult T-cell leukemia. *Leuk Res*. 2009;33(7):913-918.

Figure legends

Figure 1. Upregulation of c-Jun and JunB in ABC DLBCL cell lines is CARMA1-, MALT-1-, MyD88-, IRAK1- and TAK1- dependent. (**A**) Analysis of c-Jun, JunB and JunD protein expression and c-Jun phosphorylation on Ser 63 in GCB and ABC cell lines by Western blot. (B) Analysis of c-Jun, JunB and JunD protein expression in lysates of HBL-1 (ABC) and BJAB (GCB) cell lines transduced with control shRNA or with CARMA1-, MALT1-, IRAK1- or Myd88-specific shRNA. Silencing efficiency was assessed by Western blot analysis using anti-CARMA1, anti-MALT1, anti-IRAK1 and anti-MyD88 antibodies. (C, D) Protein expression in GCB and ABC DLBCL cell lines was determined by Western blot using the indicated antibodies. In (C), we used lysates of Jurkat cells treated with PMA and ionomycin (PI) for 1h as a positive control for MAPK activation. In (D), DLBCL cell lines of the GCB (BJAB), or ABC subtype (all others) were treated with the TAK1 inhibitor 5Z7 or with solvent alone for 24 h. In all figure panels, blotting for tubulin served as a loading control. Data are representative of at least three (A, B) or two (C, D) independent experiments.

Figure 2. Jun subunits form heterodimers with ATF2 or ATF7 in ABC DLBCL cell lines. (A) Lysates from the indicated ABC and GCB DLBCL cell lines were treated with the crosslinker BS3 or with solvent alone for 1h at 4°C. Crosslinked (open arrowheads) and non-crosslinked (filled arrowheads) proteins were revealed by Western blot using anti-c-Jun, anti-JunB and anti-JunD antibodies. (B) BS3-treated HBL-1 cell lysates were immunoprecipitated with anti-c-Jun beads or beads alone, separated by SDS-PAGE and stained with Coomassie. Proteins present in protein complexes of type I and II were analysed by mass spectrometry (MS). ATF2 and ATF7 were identified to be part of the protein complex type I, while not enough material was present in protein complex type II for MS identification. h.c., heavy chain of c-Jun. (C) Protein expression in GCB and ABC cell lines was determined by Western blot using anti-ATF2 and anti-ATF7 antibodies. (D) As in (A), but proteins were revealed using anti-ATF2 and anti-ATF7 antibodies. Grey arrowhead indicates a third, unidentified type of complex. (E) Two ABC and two GCB cell lines were lysed and proteins were precipitated using anti-c-Jun, anti-JunB, anti-JunD or anti-IRE1α antibodies (Ctr: control antibody). Proteins in lysates were analysed by Western

blotting with anti-c-Jun, anti-JunB and anti-JunD antibodies, and co-precipitating proteins (IP) with anti-ATF2 and anti-ATF7 antibodies, as indicated. (F) The composition of protein complexes of type I is schematically depicted. Data are representative of three (A and C) and two (D and E) independent experiments. Asterisks indicate a non-specific band recognized by anti-ATF7 (C and E) and migration of antibody heavy chains (E).

Figure 3. ATF3 is overexpressed and forms heterodimers with Jun subunits in ABC DLBCL cell lines. (A) Analysis of ATF3 and JDP2 protein expression in GCB and ABC cell lines was determined by Western blot using ATF3 and JDP2 antibodies. Filled arrowhead indicates the position of phosphorylated JDP2, open arrowheads indicate non-phosphorylated JDP2. (B) Immunoblot analysis of lysates of HBL-1 (ABC DLBCL) and BJAB (GCB DLBCL) cell lines, transduced with control shRNA or with CARMA1-, MALT1-, IRAK1- or MyD88-specific shRNA. Silencing efficiency was assessed by Western blot analysis using anti-CARMA1, anti-MALT1, anti-IRAK1 and anti-MyD88 antibodies. ATF2, ATF3 ATF7 protein levels were assessed by Western blot. Blotting for tubulin served as loading control in (A) and (B). (C) Lysates of indicated ABC and GCB cell lines were treated with the crosslinker BS3 or with solvent alone for 1h at 4°C. Crosslinked (open arrowheads) and non-crosslinked (filled arrowheads) proteins were assessed by Western blot using anti-ATF3 antibodies. White asterisk indicates the position of a non-specific band detected by anti-ATF3. (D) ABC DLBCL cell lines were immunoprecipitated with anti-c-Jun, anti-JunB, anti-JunD or anti-IRE1α antibodies (Ctr: control antibody). Immunoprecipitated proteins (IP) were assessed with anti-c-Jun, anti-JunB and anti-JunD antibodies, and co-precipitating proteins (co-IP) detected by anti-ATF3. *, heavy chain or light chain of the c-Jun, JunB JunD and control antibodies, filled arrowhead indicates ATF3 in the co-IP. (E) The composition of protein complexes of ATF3 with Jun family members (type 2 complexes) are depicted. Data are representative of three (A) and two (B-D) independent experiments.

Figure 4. Inhibition of AP-1 complexes impairs the viability of cell lines derived from ABC DLBCL. (A) Schematic representation of the structure of transcriptionally active Jun/ATF and inactive Jun/A-Fos complexes illustrating the dominant negative function of A-Fos. (B) Jurkat T cells were lentivirally transduced with a FLAG-

tagged expression construct for A-Fos or an empty vector (mock) as control. Cells were treated with PMA and ionomycin (PI) for the indicated times. Lysates were immunoprecipitated using anti-FLAG sepharose beads and analyzed by immunoblot with the indicated antibodies. (C) Jurkat T cells were electroporated with an IL-2 firefly luciferase reporter and a renilla luciferase reporter, stimulated with PMA and ionomycin for 14 hours and the relative luciferase activity of the cell lysates was determined. (D) Viability of ABC DLBCL and GCB DLBCL cell lines transduced with constructs co-expressing green fluorescent protein with FLAG-A-Fos (upper panel) or DN-IκBα (lower panel), assessed by flow cytometry. (E, F) HBL-1 cells were transduced with indicated silencing constructs and cell viability was assessed using PMS/MTS assay. Efficiency of protein silencing and equal loading (tubulin) was verified by Western blot. Asterisk indicates a non-specific band recognized by anti-ATF7. Three independent shRNAs were used for ATF3. (C, E and F) Bars represent means ± SD; differences were statistically significant with $^{**}P < 0.01$, $^{***}P < 0.001$ (unpaired t-test). Data in figure panels (B-E) are representative of at least two independent experiments.

Figure 5. Strong nuclear ATF3 expression is a hallmark of non-GC and ABC DLBCL patients. (A) Relative mRNA expression of ATF2, -3 and -7 in ABC versus GCB DLBCL biopsies. Error bars indicate SEMs. (B) Immunofluorescence staining of ATF3 expression and localization in the indicated GCB and ABC DLBCL cell lines. Bar: 5 μm. (C) Histological staining of ATF3 expression in representative biopsy samples of DLBCL patients. Bar: 50 μM, magnification 400x. (D, E) Tissue microarray (TMA) analysis of DLBCL biopsies previously categorized into GCB or non-GC using the Hans algorithm (D), or into ABC or GCB by GEP (E). Bar graphs summarizing the classification of non-GC and GCB patients (D) or ABC and GCB patients (E) according to staining intensity (weak, intermediate and strong) and subcellular localization of ATF3 (C: cytoplasmic, N: partially or predominantly nuclear). Analysis was performed on 28 (D) or 17 (E) patients with nodal (lymph node) tumors.

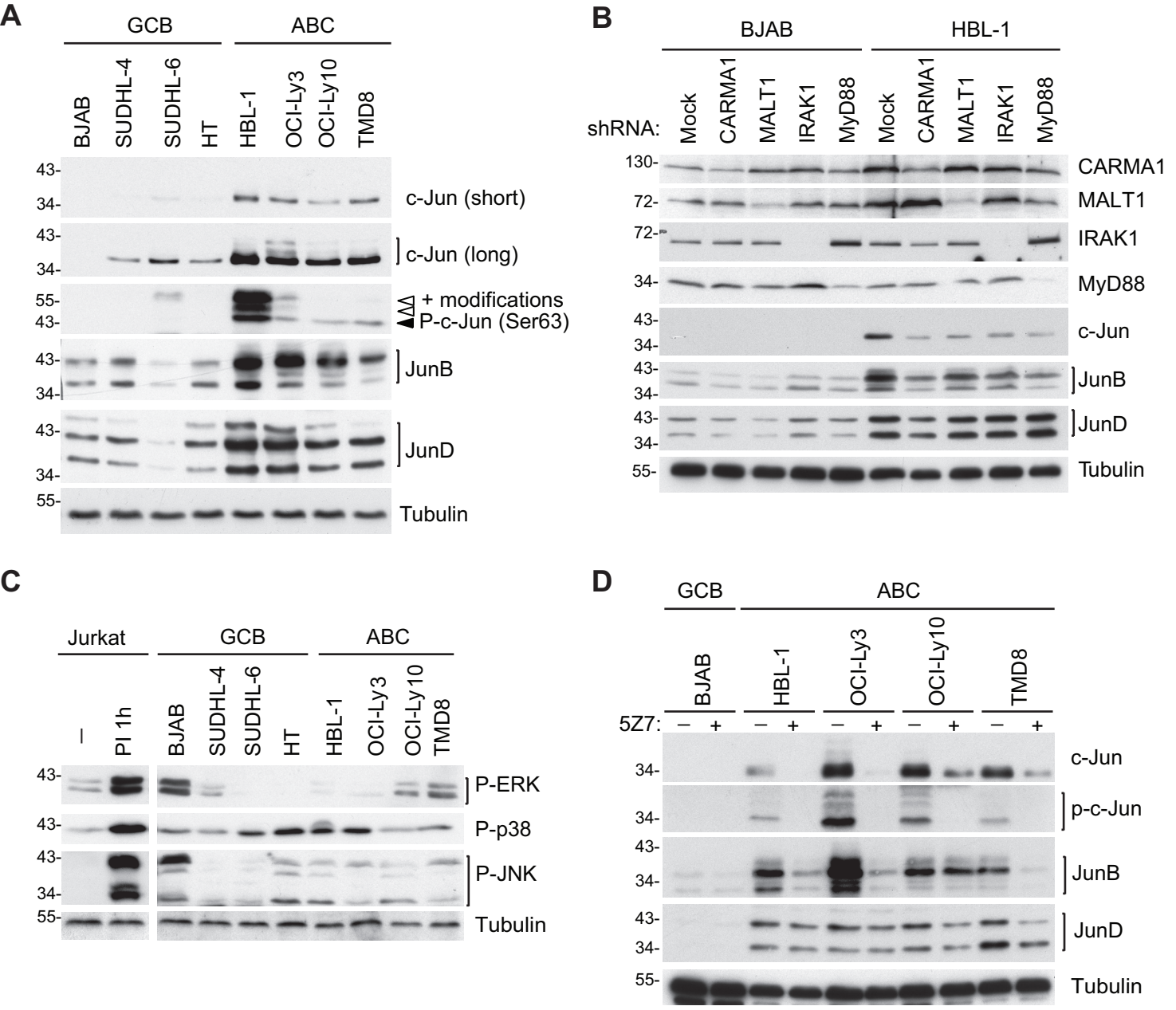

Juilland et al., Figure 1

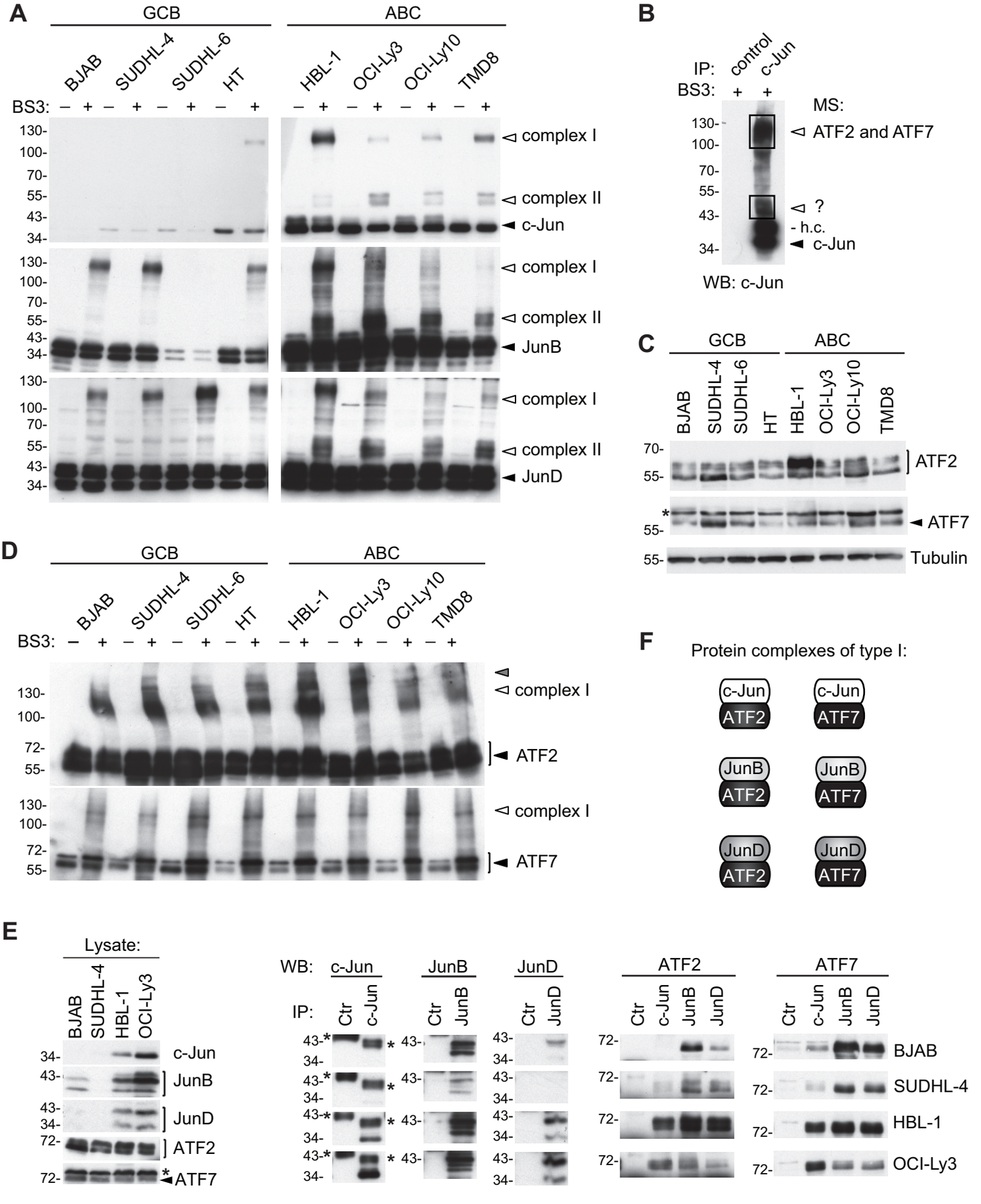

Juilland et al., Figure 2

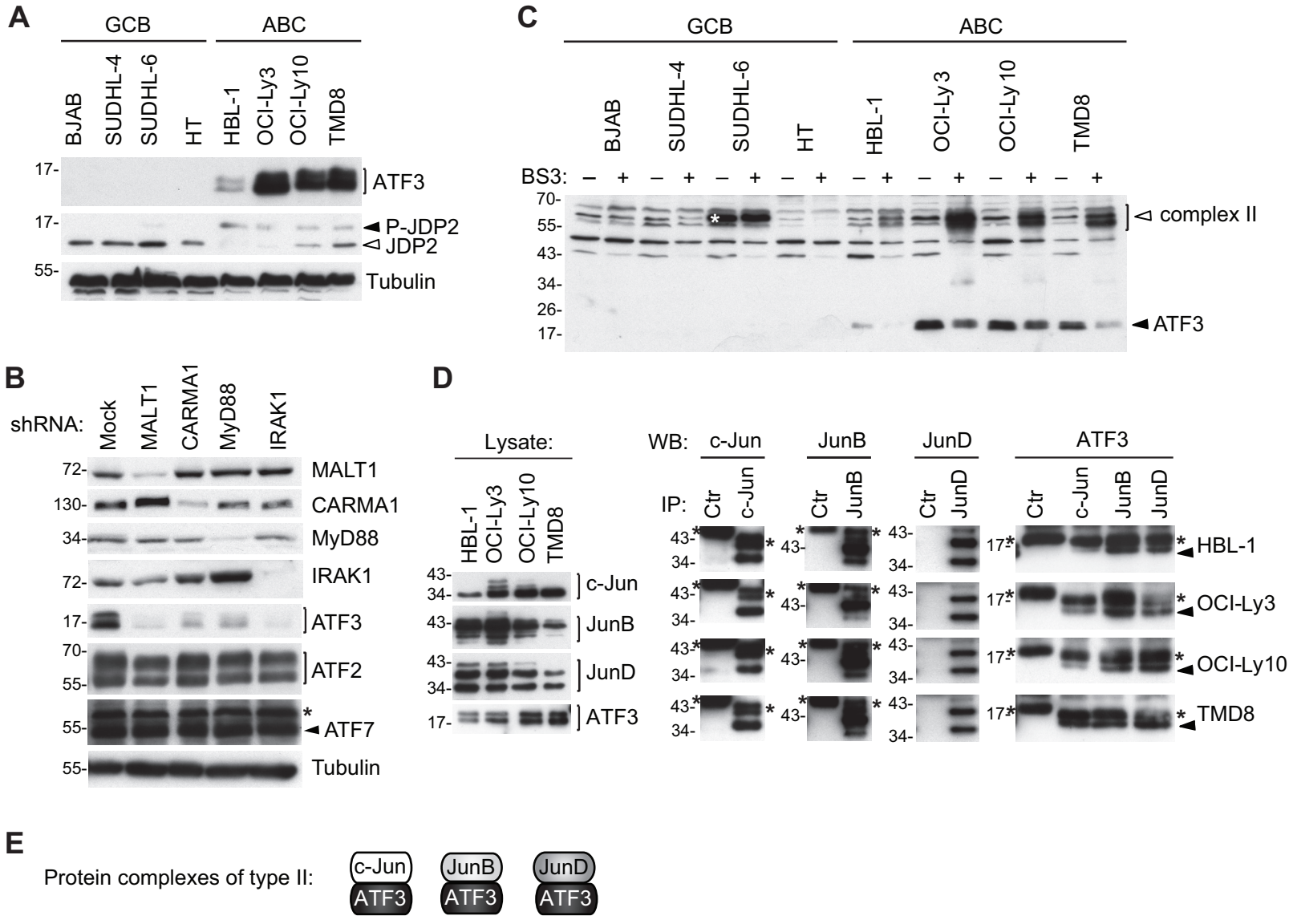

Juilland et al., Figure 3

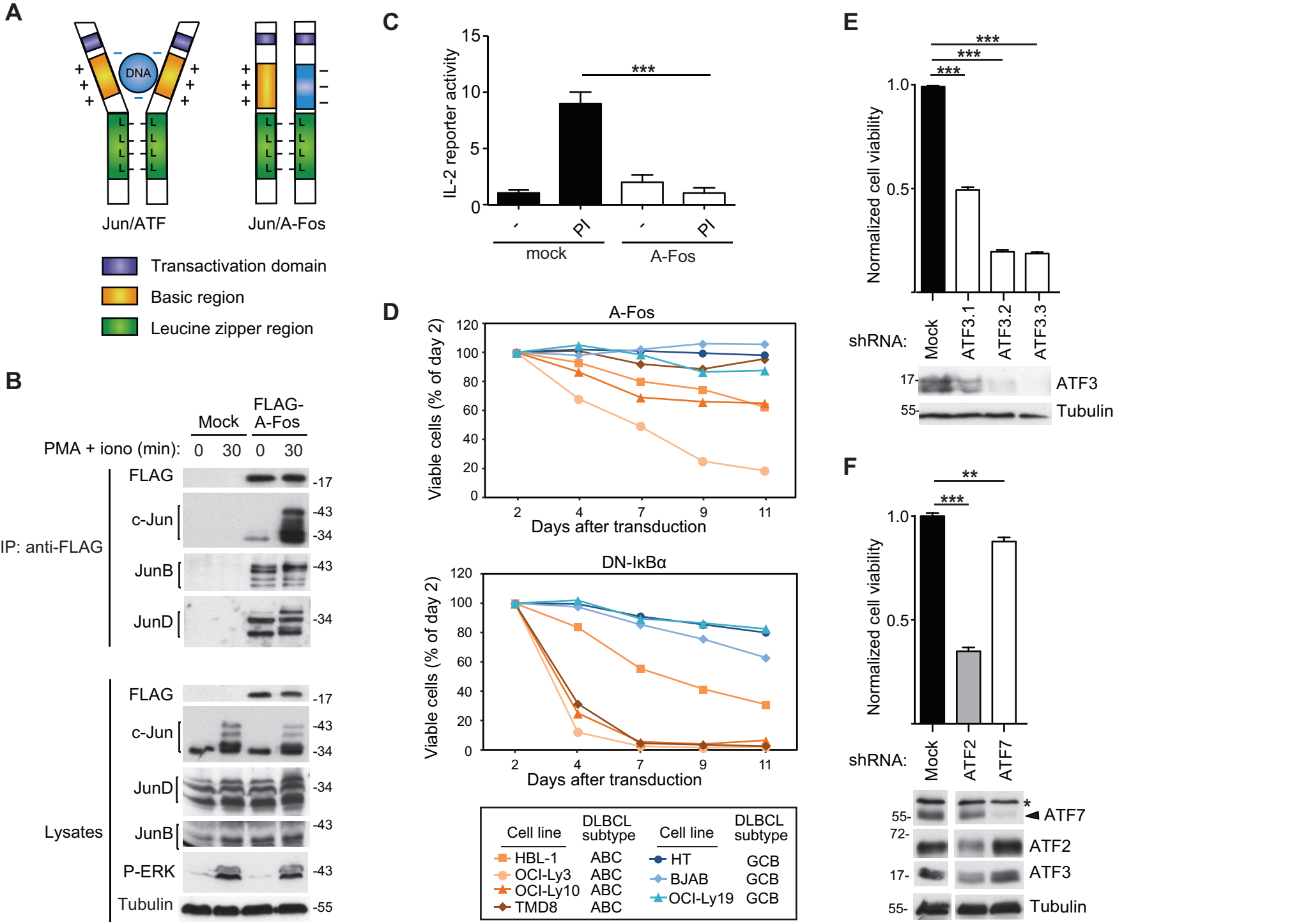

Juilland et al., Figure 4

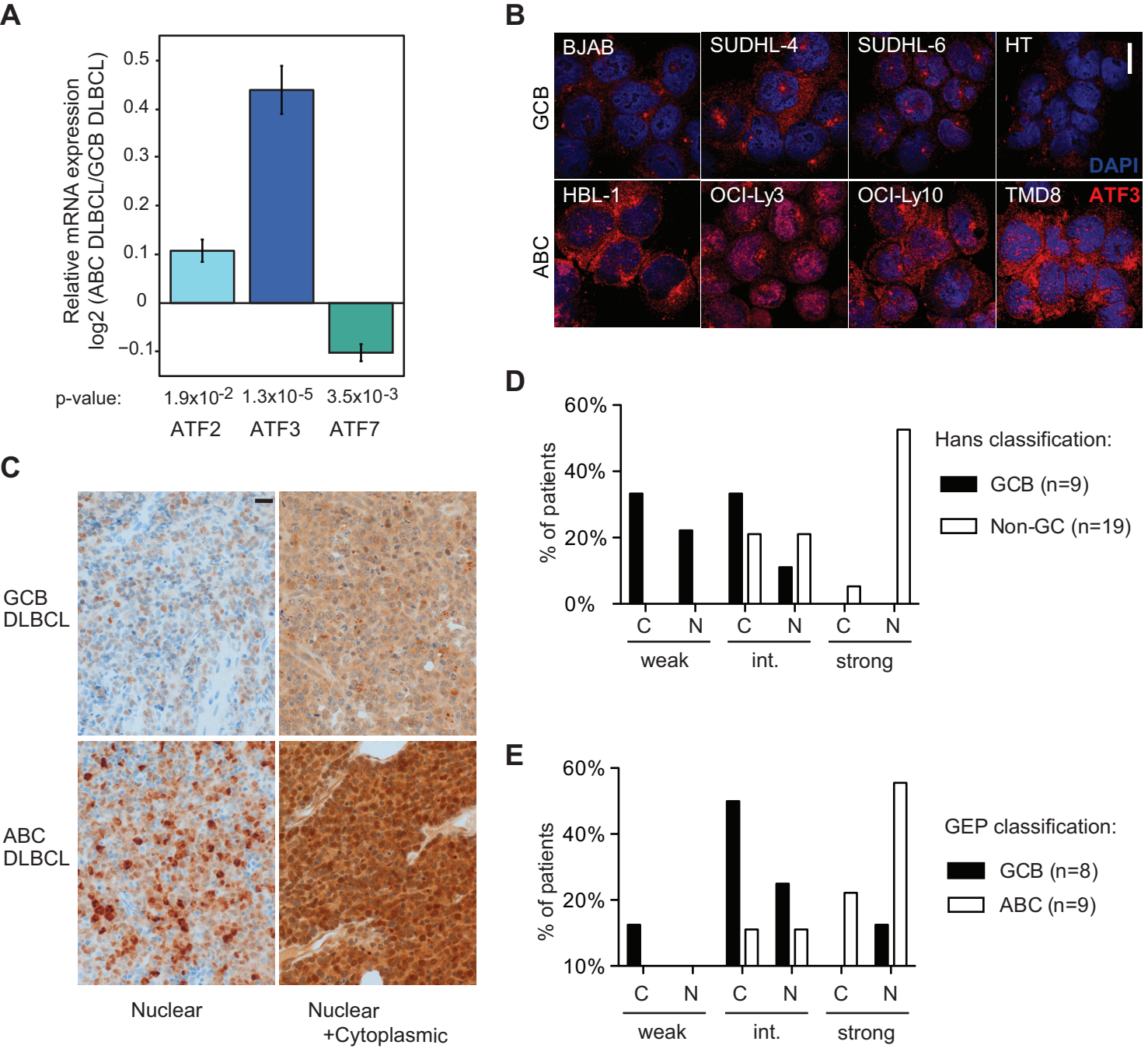

Juilland et al., Figure 5

CARMA1- and MyD88-dependent activation of specific AP-1 complexes is a hallmark of ABC diffuse large B-cell lymphomas

Mélanie Juilland, Montserrat Gonzalez, Tabea Erdmann, Yara Banz, Zala Jevnikar, Stephan Hailfinger, Alexandar Tzankov, Michael Grau, Georg Lenz, Urban Novak and Margot Thome

Supplemental methods

Plasmids

The FLAG-A-Fos sequence was obtained from Addgene (Plasmid 33353) and subcloned into the retroviral vector pMSCV-IRES-GFP.[27] The following lentiviral vectors (pLKO.1) were used for ATF2, ATF7, ATF3, c-Jun, IRAK1 and MyD88 silencing in DLBCL cell lines: ATF2 shRNA (TRCN0000229648), and ATF3 (TRCN0000013568, TRCN0000013571, TRCN0000013572), ATF7 (TRCN0000017116), c-Jun shRNA (TRCN0000039590), IRAK1 shRNA (TRCN0000000544) and MyD88 (TRCN0000008024). For silencing of MALT1 and CARMA1, cells were transduced with a lentiviral vector (pAB286.1, a kind gift of R. Iggo, Bordeaux, France) containing short hairpin RNA sequences specific for CARMA1 (5'-GCTATGATTTCTCTTGCAT-3') or MALT1 (5'-GTCACAGAATTGAGTGATTTC-3').[7]

Antibodies

Antibodies against Tubulin (B-5-1-2), FLAG (M2) and P-ERK (MAPK-YT) were from Sigma; c-Jun (60A8), JunB (C37F9), JunD (D17G2), ATF2 (20F1), P-p38 (D3F9), JNK and P-IκBα (5A5) antibodies were from Cell Signaling, and ATF3 (C-19), MyD88 (E-11), IRAK1 (H-273) and P-c-Jun (KM-1) antibodies were from Santa Cruz Biotechnology. Other antibodies used were specific for CARMA1 (AL220; Alexis), P-JNK (Invitrogen), ATF7 (NBP1-30071, Novus Biologicals) and JDP2 (Abcam Ab40916). Affinity-purified anti-MALT1 has been reported.[27,28] Horseradish peroxidase-coupled goat anti-mouse (115-035-146) and anti-rabbit (111-035-144) were from Jackson ImmunoResearch.

Analysis of c-Jun binding partners by mass spectrometry

Large-scale immunoprecipitation with anti-c-Jun coupled to protein G Sepharose beads or protein G Sepharose beads was performed on cross-linked HBL-1 lysates,

followed by SDS-PAGE and staining with colloidal Coomassie (Invitrogen). The bands corresponding to complexes of type I and II were excised. Proteins were in-gel reduced with DTT, alkylated with iodoacetamide and digested with sequencing-grade trypsin. Extracted peptides were analyzed by nanoflow liquid chromatography–tandem mass spectrometry on a LTQ-Velos PRO orbitrap mass spectrometer (Thermo Fisher Scientific). Tandem mass spectra of peptides were searched with MASCOT (Matrix Science, London) against the UniProtKB protein sequence database. Identifications were filtered with Scaffold (Proteome Sciences, Portland, Oregon) to have a minimum of 95% probability and two peptides. The ten most abundant proteins in the 40-60 and 100-150 kD mass ranges that were identified by this approach are listed in the supplemental Table 1.

Immunofluorescence Microscopy

Lymphoma cells were cytospinned for 6 min at 900 rpm to Superfrost®Plus microscope slides (Thermo Scientific). Slides were washed with PBS, the cells fixed with ice cold methanol for 30 min and permeabilized with 0.1 % Triton X-100 in PBS for 15 min. Nonspecific staining was blocked with 1 % BSA in PBS overnight at 4°C. Next, the slides were incubated with anti-ATF3 antibody (1:50) in 1 % BSA for 2 h at room temperature. Cells were washed with PBS and stained with labeled F(ab')2 antibody fragments for 1 h. After washing with PBS, DAPI-containing ProLong antifade kit (Molecular Probes) was mounted on dried slides to visualize DNA and protect the slides from bleaching. Fluorescence microscopy was performed using Carl Zeiss LSM 510 confocal microscopes and the images were analyzed by Carl Zeiss LSM or ZEN 2007 image software.

Cell viability assay

72 h after infection, transduced DLBCL cells were selected with puromycin (1 ug/ml) for 24 h, and silencing efficiency was determined by western blot. Cells were replated at the same concentration, and cell viability was assessed 5 days later using MTS (Promega, 400 µg/mL) and PMS (Sigma, 9 µg/mL), according to the manufacturer's instructions. Reduction of MTS to formazan was measured at 492 nm with Capture 96 Software on a LEDETECT 96 microplate spectrophotometer (Dynamica).

Supplemental table

Table S1: List of the 10 most abundant c-Jun binding proteins identified by mass spectrometry. The number of independently identified peptides for each sample is indicated.

			HBL-1 IP Ctr	HBL-1 IP Ctr	HBL-1 IP c-Jun	HBL-1 IP c-Jun
#	Identified Proteins	Molecular Weight	gel slice 100-150 kDa	gel slice 40-60 kDa	gel slice 100-150 kDa	gel slice 40-60 kDa
1	FBX38	134 kDa	0	0	20	0
2	c-Jun	36 kDa	0	0	9	3
3	CKAP5	226 kDa	0	0	9	0
4	ATF7	53 kDa	0	0	7	0
5	ATF2	55 kDa	0	0	6	1
6	ACTZ	43 kDa	0	0	3	0
7	ITB1	88 kDa	0	0	3	0
8	NOLC1	74 kDa	0	0	3	0
9	MKL1	99 kDa	0	0	3	0
10	EIF3G	36 kDa	0	0	2	0

Supplemental figures

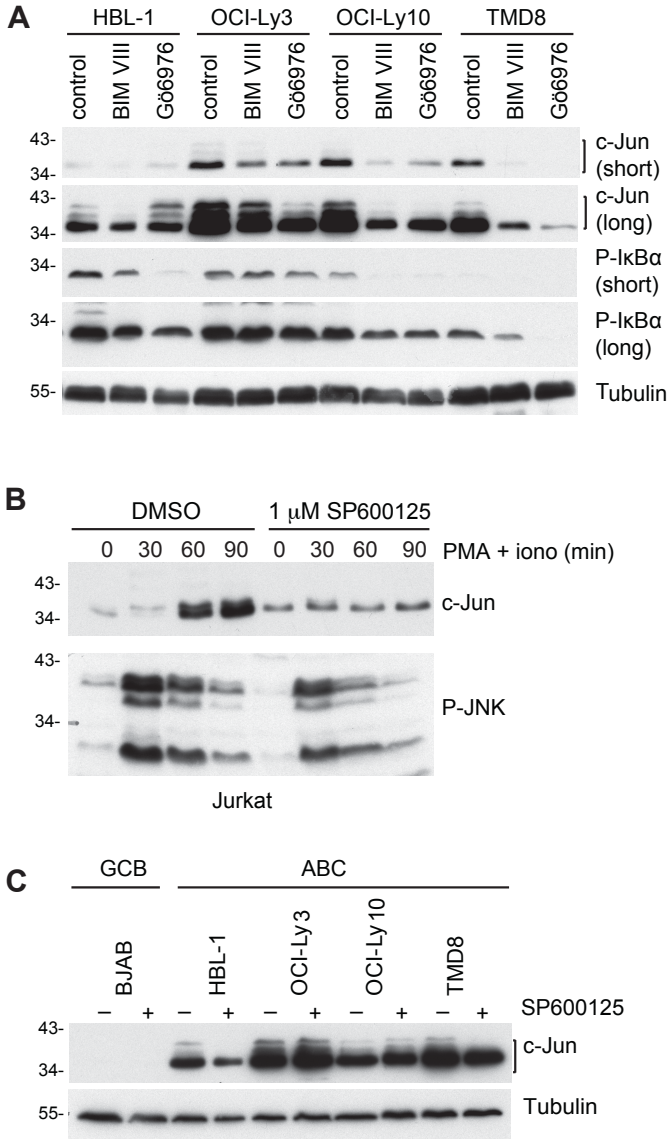

Figure S1. JNK inhibition efficiently blocks c-Jun upregulation in stimulated Jurkat T cells.
(A) DLBCL cell lines of the ABC type were treated with the PKC inhibitors BIM VIII or Gö6976 or with solvent control for 24 h, and c-Jun protein expression was assessed by Western blot. Efficiency of PKC inhibition was assessed by blotting for IkBα phosphorylation. Blotting for tubulin served as a loading control. (B) Western blot analysis of cell lysates from Jurkat T cells that were pretreated for 30 min with either 1μM of the JNK inhibitor SP600125 or solvent alone and then stimulated using PMA and ionomycin for the indicated times. (C) DLBCL cell lines of the GCB (BJAB), or ABC subtype (all others) were treated with the JNK inhibitor SP600125 or with solvent alone for 24 h, and c-Jun expression was assessed by Western blot. Blotting for tubulin served as a loading control. Data in all figure panels are representative of two independent experiments.

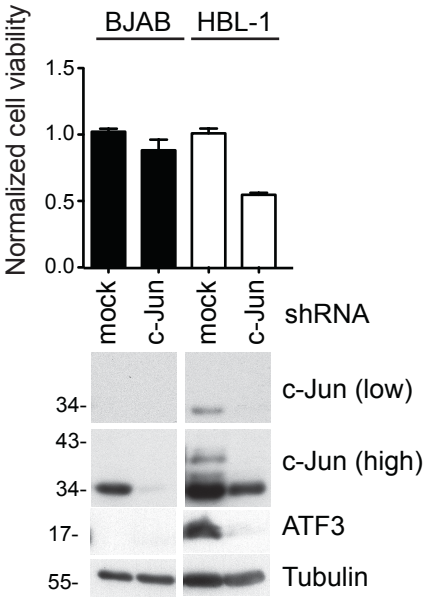

Figure S2. Silencing of c-Jun affects ATF3 expression and HBL-1 cell viability. DLBCL cell lines of the GCB (BJAB) or ABC (HBL-1) subtype were transduced with a c-Jun-specific or control shRNA and cell viability and protein expression were assessed using PMS/MTS assay and Western blot. Blotting for tubulin was used as a loading control. Data are representative of two independent experiments.

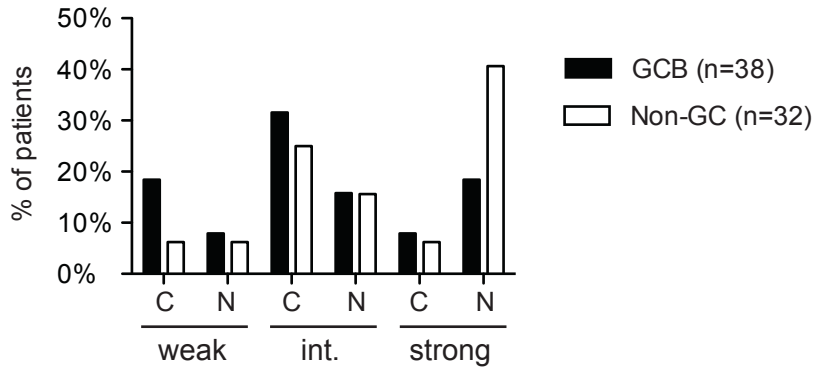

Figure S3. Analysis of ATF3 expression in DLBCL tissue microarrays. Tissue microarray analysis of DLBCL biopsies previously categorized into GCB and non-GC using the Hans algorithm. Bar graphs are summarizing the classification of non-GC and GCB patients according to staining intensity (weak, intermediate and strong) and subcellular localization of ATF3 (C: cytoplasmic, N: partially or entirely nuclear). Analysis was performed on all 70 samples available from patients with extra-nodal or nodal (lymph node) tumors.